time dependence of activation and require prolonged periods (minutes) for recovery between depolarizing steps.
18. P. R. Stanfield, *Rev. Physiol. Biochem. Pharmacol.* **97**, 1 (1983); G. Yellen, *Annu. Rev. Biophys. Biophys. Chem.* **16**, 227 (1987).
19. R. MacKinnon and G. Yellen, unpublished data.
20. L. Stryer, *Biochemistry* (Freeman, New York, ed. 3, 1988).
21. A. L. Hodgkin and R. D. Keynes, *J. Physiol. (London)* **128**, 61 (1955); P. Horowicz, P. W. Gage, R. S. Eisenberg, *J. Gen. Physiol.* **51**, 193s (1968); B. Hille and W. Schwarz, *ibid.* **72**, 409 (1978); T. B. Begenisich and P. DeWeer, *ibid.* **76**, 83 (1980); B. C. Spalding, O. Senyk, J. G. Swift, P. Horowicz, *Am. J. Physiol.* **241**, c68 (1981).
22. Experiments with bis-quaternary ammonium blockers [A. Villarroel, O. Alvarez, A. Oberhauser, R. Latorre, *Pfluegers Arch.* **413**, 118 (1988)] indicate that 27% of the electric potential falls across a physical distance of about 10 Å. If the potential falls linearly over the narrow region of the pore, then 80% of the potential would fall across a distance of about 30 Å.
23. Mutagenesis, RNA synthesis, oocyte injection, voltage-clamp and patch-clamp methods are as described [R. MacKinnon, P. Reinhart, M. M. White, *Neuron* **1**, 997 (1988); (*5*)].
24. We thank L. Heginbotham and P. Hess for helpful comments on the manuscript. G.Y. is a Howard Hughes Medical Institute investigator. R.M. was supported by NIH research grant GM4399.

21 November 1990; accepted 18 January 1991

Exchange of Conduction Pathways Between Two Related K^+ Channels

HALI A. HARTMANN, GLENN E. KIRSCH, JOHN A. DREWE, MAURIZIO TAGLIALATELA, ROLF H. JOHO, ARTHUR M. BROWN

The structure of the ion conduction pathway or pore of voltage-gated ion channels is unknown, although the linker between the membrane spanning segments S5 and S6 has been suggested to form part of the pore in potassium channels. To test whether this region controls potassium channel conduction, a 21–amino acid segment of the S5-S6 linker was transplanted from the voltage-activated potassium channel NGK2 to another potassium channel DRK1, which has very different pore properties. In the resulting chimeric channel, the single channel conductance and blockade by external and internal tetraethylammonium (TEA) ion were characteristic of the donor NGK2 channel. Thus, this 21–amino acid segment controls the essential biophysical properties of the pore and may form the conduction pathway of these potassium channels.

VOLTAGE-GATED ION CHANNELS are thought to consist of four similar domains forming a central pore (*1–4*) with each repeat consisting of six transmembrane segments, S1 to S6 (Fig. 1A). The linker region connecting S5 and S6 is highly conserved, especially in K^+ channels, and therefore seemed a candidate for the conduction pathway of K^+ channels (*2, 3, 5, 6*). In support of this notion is evidence that point mutations in the S5-S6 loop of the Shaker K^+ channel (*7, 8*) changed the blockade produced by a large peptide toxin charybdotoxin (7) and the small, open channel blocker TEA (*8, 9*), and also changed single channel conductance (*8*). To test the role of the S5-S6 linker in forming the channel pore we took advantage of the differences in pore properties of two related K^+ channels DRK1 (*10*) and NGK2 (*11*). The single channel conductance of NGK2 is almost three times that of DRK1, and NGK2 was more sensitive to blockade by TEA applied to the external side of the membrane whereas DRK1 was more sensitive to blockade by TEA applied to the internal side of the membrane. We attempted to modify these properties of the channel by exchanging the S5-S6 loop between the two K^+ channels. To do this, we introduced silent restriction endonuclease sites into DRK1, which allowed removal of a 21–amino acid segment in the S5-S6 linker region, and then generated a chimeric channel in which the corresponding segment was transferred from NGK2 to DRK1 (Fig. 1B) (*12*). If this segment constituted the pore, our prediction was that the chimeric channel should have the conductance and TEA blocking profile of the donor NGK2 channel.

When the chimeric DRK-NGK channel was expressed in oocytes (*13*) the unitary currents at a test potential of 0 mV were about three times greater than those of DRK1 (Fig. 2A). The slope conductance measured over the test potential range of −10 to +40 mV was also about three times greater than that of DRK1 (Fig. 2B). At test potentials outside this range, some curvature was apparent in the single channel current-voltage (*I-V*) relation of DRK1, a result consistent with the outward rectification in the instantaneous *I-V* curve obtained from macroscopic current recordings (*10*). By contrast, no curvature was apparent for DRK-NGK or NGK2, and the extrapolated reversal potential from the single channel *I-V* relation agreed with that expected for a K^+-selective channel.

TEA blocked the chimeric channel in a manner that mimicked TEA blockade of NGK2 and was different from TEA blockade of DRK1. Extracellular TEA at 3.0 mM produced a weak blockade of DRK1 whole-cell currents, a strong blockade of NGK2 currents, and a strong blockade of DRK-NGK currents. By contrast, intracellular TEA at 0.3 mM produced a strong blockade of DRK1 currents, a weak blockade of NGK2 currents, and a weak blockade of DRK-NGK currents (Fig. 3). The differences among the concentration-response curves for extracellular and intracellular TEA blockade of DRK1, NGK2, and DRK-NGK are shown in Fig. 4. Whereas the internal TEA blockade of the chimeric channel was indistinguishable from that for NGK2, the concentration-response curve for external blockade appeared to be intermediate between that of DRK1 and NGK2.

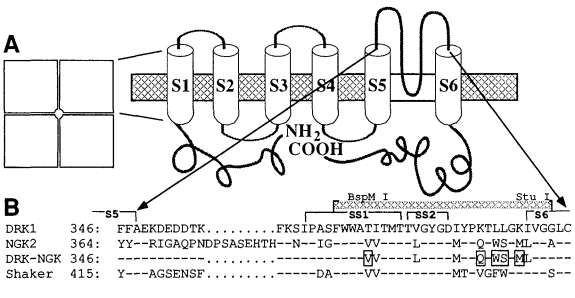

Fig. 1. Construction of a chimeric K^+ channel. (**A**) Model of the topography of a voltage-gated K^+ channel. On the left are four identical subunits arranged about a central pore. On the right is a single subunit with its six putative transmembrane segments and their connecting loops. The loop between S5 and S6 is placed in the membrane to explain the results obtained in this paper. (**B**) Comparison among DRK1, NGK2, the DRK-NGK, and Shaker K^+ channels of the amino acid sequences in the S5-S6 loop. The dashes represent residues identical to DRK1. The dots represent interruptions that maintain the alignment with NGK2. The numbers apply to the first residue in each of the aligned sequences. The cross-hatched bar between the BspM I and Stu I restriction sites indicates the extent of the restriction fragment in DRK1 that was replaced. SS1 and SS2 are two short segments thought to span part of the membrane (*5*). The boxed residues in the chimeric segment are nonconservative differences between NGK2 and DRK1.

H. A. Hartmann, J. A. Drewe, M. Taglialatela, R. H. Joho, A. M. Brown, Department of Molecular Physiology and Biophysics, Baylor College of Medicine, One Baylor Plaza, Houston, TX 77030.
G. E. Kirsch, Departments of Molecular Physiology and Biophysics and Anesthesiology, Baylor College of Medicine, One Baylor Plaza, Houston, TX 77030.

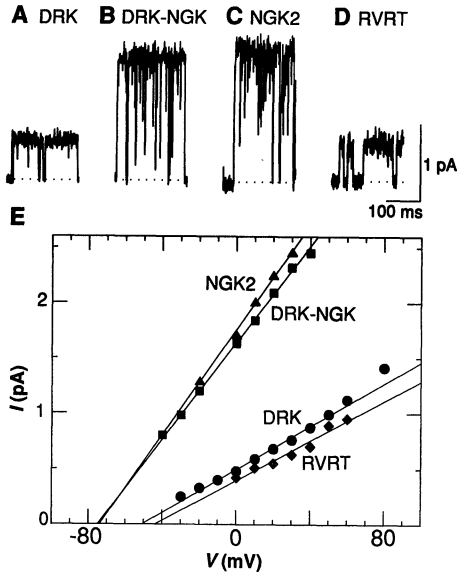

Fig. 2. Comparison of representative single channel currents of DRK1 (**A**), the chimera DRK-NGK (**B**), NGK2 (**C**), and the revertant of DRK-NGK to DRK1 (RVRT) (**D**). Holding potential was −100 mV, pulses were 215 ms in duration, and the pulse frequency was 0.3 Hz. Currents were low-pass filtered at 0.5 kHz. The length of each trace (A through D) coincides with the duration of the test pulse. (**E**) Single channel *I-V* plots representative of each clone. For NGK2, DRK-NGK, DRK1, and RVRT the slope conductances between −10 and +40 mV were (mean ± SEM) 21.8 ± 0.7 (n = 8), 21.5 ± 0.5 (n = 11), 8.1 ± 0.3 (n = 10), and 8.4 ± 0.6 (n = 4), respectively; n is the number of patches. The values from three different batches of oocytes were the same.

The sites at which TEA produced blockade were further defined by considering the effects of membrane potential on blockade. Internal TEA blockade became stronger at more positive potentials, a result similar to that for internal TEA blockade in squid giant axons (*14*). On the other hand external blockade was not affected by membrane potential (*15*). From these results we infer the presence of two binding sites for TEA; one at the external mouth of the pore outside of the membrane field and the other at a site about 4/5 of the electrical distance inward from the external mouth. Similar external and internal binding sites for TEA occur in delayed rectifier K^+ channels in vertebrate myelinated axons (*16, 17*) and molluscan neurons (*18, 19*).

Although our results suggested that the substituted stretch of 21 amino acids determined ion permeation and TEA sensitivity, there was the possibility that unintended alterations in the remaining part of the cDNA molecule were fully or partially responsible for the change in phenotype. To exclude this possibility, we used the chimeric cDNA to generate a revertant K^+ channel construct with the original sequence of DRK1. The BspM I–Stu I fragment from the chimeric channel was removed and replaced with the BspM I–Stu I fragment from DRK1. The resulting revertant cDNA expressed single channel and whole cell K^+ currents in oocytes that were indistinguishable from those generated by the original DRK1 cDNA (Fig. 2, D and E). The profile of TEA blockade was also restored to that characteristic of DRK1 (Fig. 4). These results show that the change in phenotype of the chimeric channel was due to substitution of the BspM I–Stu I fragment.

Although the chimeric channel had the same conductance and nearly the same TEA blocking profile as the donor NGK2 channel, other properties not generally attributable to the pore itself were changed. The rate at which whole-oocyte currents activated after a step change in potential was slower than for either donor NGK2 or host DRK1 (Fig. 3), and activation occurred at more negative potentials. The slowing and the shift in activation may have resulted from an interaction between the substituted segment and the remainder of the host DRK1 channel.

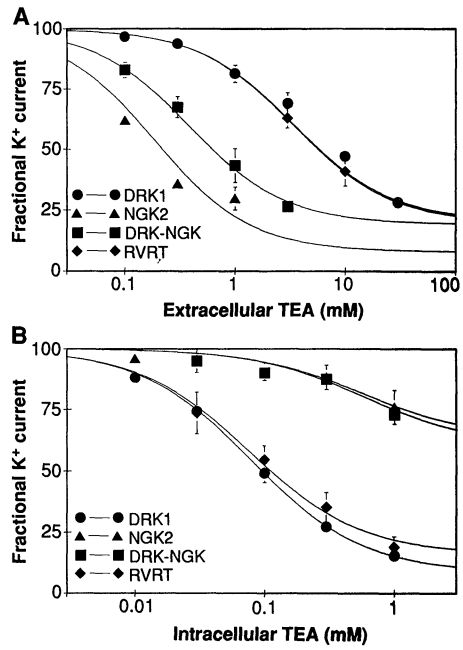

Fig. 4. Comparison of the concentration-response curves for external and internal TEA blockade of DRK1, NGK2, DRK-NGK, and RVRT. Fractional K^+ current was calculated as 100 × I_{TEA}/I_{CONT}. Both currents were measured at the end of a 350-ms pulse to +50 (DRK1, NGK2, and RVRT) or +20 (DRK-NGK) mV from a holding potential of −80mV. Each data point is the mean ± SEM of at least three and at most six determinations in oocytes from three different batches. Solid lines, best fits for a one-to-one drug receptor binding scheme.

Our results have identified a 21–amino acid segment in the S5-S6 linker of two related K^+ channels that controls the external and internal binding sites for TEA blockade and the conductance or rate of perme-

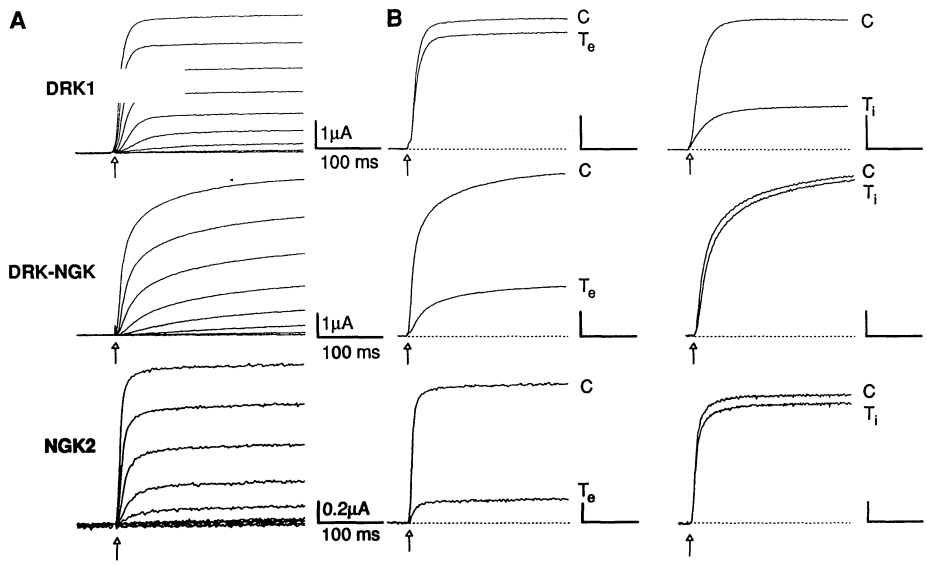

Fig. 3. TEA blockade of whole-oocyte currents expressing DRK1, DRK-NGK, and NGK2. (**A**) Representative families of currents generated by each clone. Holding potential was −80 mV, and test potentials were applied in 10-mV steps beginning with −40 mV (DRK1, NGK2) or −50 mV (DRK-NGK). The most depolarized potentials were +50 mV (DRK1, NGK2) or +20 mV (DRK-NGK). The pulses were 350 ms in duration and were applied at 0.1 Hz. Arrows indicate the beginning of each depolarizing test pulse. DRK-NGK currents activated more slowly than currents from either DRK1 or NGK2. (**B**) Representative effects of external (T_e) and internal TEA blockade (T_i). The control (C) currents were produced by voltage-clamp steps from −80 mV to +50mV (DRK1, NGK2) or +20 mV (DRK-NGK). The effects of external and internal TEA were measured 3 min after application by superfusion or intracellular injection of TEA at concentrations of 3 mM and 0.3 mM, respectively.

ation of K^+. Our results complement experiments in which (i) point mutations at several amino acids in a corresponding segment of the S5-S6 loop of the Shaker K^+ channel changed external blockade by TEA (*8*); (ii) several mutations at one amino acid, T449, changed both TEA blockade and inward single channel conductance (*8*); and (iii) a mutation at T441 greatly reduced internal TEA blockade (*20*). Because of the concurrence of the conclusions from point mutation experiments and our experiments with the chimeric channel, it is unlikely that either result is caused by an unintended structural change induced by the mutation. The extensive changes induced by the chimeric exchange are, in any case, not easily explained by a structural effect because three pronounced characteristics of the donor phenotype were transferred nearly unaltered.

Of the 21 amino acids in the transplanted region, there are nine differences between NGK2 and DRK1 and five of them (Fig. 1B) are nonconservative substitutions. Of these, the Q at position 409 of NGK2 corresponding to K382 in DRK1 is especially interesting because on electrostatic grounds it could account for the differences between DRK1 and NGK2 in external TEA blockade and rectification. The neighboring Y at position 407 of NGK2 corresponds to T449 of Shaker, which is known to be important for external TEA blockade and single channel conductance (*8*).

Functional experiments led to the prediction that the pore of voltage-gated ion channels would have dimensions accommodating one or two ions and a few water molecules (*21*). The results with point mutations (*8*) and our results with the chimeric channel indicate that the pore may be determined by a stretch of 21 amino acids. If this region forms an α-helical hairpin it would have a length of about 15 Å, and the 30 Å thick membrane would therefore have to be constricted in the pore region. Another possibility that is more compatible with the membrane thickness is that this stretch of amino acids forms two antiparallel β-strands that could traverse the membrane.

REFERENCES AND NOTES

1. M. Noda *et al.*, *Nature* **320**, 188 (1986).
2. H. R. Guy and P. Seetharamulu, *Proc. Natl. Acad. Sci. U.S.A.* **83**, 508 (1986).
3. R. E. Greenblatt *et al.*, *FEBS Lett.* **193**, 125 (1985).
4. W. A. Catterall, *Science* **242**, 50 (1988).
5. H. R. Guy and F. Conti, *Trends Neurosci.* **13**, 201 (1990).
6. B. L. Tempel *et al.*, *Science* **237**, 770 (1987).
7. R. MacKinnon and C. Miller, *ibid.* **245**, 1382 (1989).
8. R. MacKinnon and G. Yellen, *ibid.* **250**, 276 (1990).
9. C. M. Armstrong and L. Binstock, *J. Gen. Physiol.* **48**, 859 (1965).
10. G. C. Frech, A. M. J. VanDongen, G. Schuster, A. M. Brown, R. H. Joho, *Nature* **340**, 642 (1989).
11. S. Yokoyama *et al.*, *FEBS Lett.* **259**, 37 (1989). The NGK2 clone was isolated from a rat brain cDNA library and is the rat homolog of the NG108 isolate.
12. The BamH I restriction fragment (position 906 and 1516 in the coding region) was excised from DRK1 and subcloned into M13mp19. Silent restriction sites for BspM I (C to A and C to T change at positions 1080 and 1083, respectively) and Stu I (G to A and G to C change at positions 1170 and 1173, respectively) were introduced [J. R. Moorman *et al.*, *Science* **250**, 688 (1990)]. The BamH I fragment was ligated back into DRK1, and the extent of the fragment was sequenced. cRNA run-off transcripts were prepared and microinjected into *Xenopus* oocytes [R. H. Joho *et al.*, *Mol. Brain Res.* **7**, 105 (1990); A. M. J. VanDongen *et al.*, *Neuron* **5**, 433 (1990)]. In oocytes the cRNA for DRK1 directed the expression of whole-cell and single channel currents that were indistinguishable from those for the parent DRK1. NGK2 (*11*) was cloned from a rat brain cDNA library (*10*). In oocytes cRNA directed expression of whole-cell and single channel currents that were identical to those from NG108 cells. The DNA segment in DRK1 corresponding to the region encoding amino acids 364 through 390 was replaced with the DNA segment encoding amino acids 391 through 417 of NGK2. Because the first four and the last two amino acids of the substituted restriction fragment were identical to those of DRK1, the chimeric region actually extended over 21 amino acids. The NGK2 segment to be exchanged was synthesized by the polymerase chain reaction (PCR) technique [H. A. Erlich, Ed., *PCR Technology* (Stockton Press, New York, 1989)] with forward 5′-ATATACCTGCCGGCTTCTGGTGGGCTGTGGT) and reverse (5′-GCACAGGCCTCCCACCAACATCCCAGACCA) primers encoding at their 5′ ends a BspM I and a Stu I site, respectively. The recognition sites were preceded by four extra nucleotides to allow efficient restriction enzyme digestion of the PCR product for cloning into DRK1 that had been cut with BspM I and Stu I. The construct was verified by restriction mapping and sequencing. cRNA run-off transcripts were prepared and microinjected as above.
13. Whole-cell recording from Stage V–VI *Xenopus* oocytes was performed and analyzed as described [A. M. J. VanDongen *et al.*, *Neuron* **5**, 433 (1990)] except that the potential electrode was filled with 120 mM potassium methanesulfonate (MES), 2 mM $MgCl_2$, 10 mM Hepes, and 50 mM TEACl (pH 7.2). TEACl was substituted for NMDGMES in the external solution as necessary. To inject TEA, a pneumatic pressure ejector (Picospritzer II, General Valve Corp.) was connected to the potential electrode. The volume injected was estimated from the volume of the fluid droplet expelled in air with the pipet tip prior to and after penetration of the oocyte [I. Parker and R. Miledi, *Proc. R. Soc. London B* **228**, 307 (1986)]. The volume was always less than 2% of the oocyte volume. Injection of equal amounts of TEA-free vehicle was without effect. The experiments were performed at 21°C. Single channel currents were recorded and analyzed as described [J. R. Moorman *et al.*, *Neuron* **4**, 243 (1990)]. The pipet solution was 120 mM NaCl, 2.5 mM KCl, 2 mM $MgCl_2$, 10 mM Hepes, pH 7.2. A bath solution that depolarized the membrane to 0 mV was used and was 100 mM KCl, 10 mM EGTA, 10 mM Hepes, pH 7.2.
14. C. M. Armstrong. *J. Gen. Physiol.* **58**, 413 (1971).
15. M. Taglialatela *et al.*, manuscript in preparation.
16. E. Koppenhöfer and W. Vogel, *Pfluegers Arch.* **313**, 361 (1969).
17. C. M. Armstrong and B. Hille, *J. Gen. Physiol.* **59**, 388 (1972).
18. S. H. Thompson, *J. Physiol (London)* **265**, 465 (1977).
19. A. Hermann and A. L. F. Gorman, *Neurosci. Lett.* **12**, 87 (1979).
20. G. Yellen, M. Jurman, T. Abramson, R. MacKinnon, *Science* **251**, 939 (1991).
21. B. Hille, *Ionic Channels of Excitable Membrane* (Sinauer, Sunderland, MA, 1984).

22. We thank S. Verma for cloning the rat brain homolog of NGK2, G. Schuster for oocyte management, and D. Witham and J. Breedlove for their secretarial assistance. Supported in part by National Institutes of Health grants NS23877 to A.M.B., NS28407 to R.H.J., and NS08805 to J.A.D., American Heart Association–Texas Affiliate 89R197 to G.E.K., and the Italian National Research Council (CNR) to M.T.

12 December 1990; accepted 22 January 1991

Reshaping the Cortical Motor Map by Unmasking Latent Intracortical Connections

KIMBERLE M. JACOBS AND JOHN P. DONOGHUE

The primary motor cortex (MI) contains a map organized so that contralateral limb or facial movements are elicited by electrical stimulation within separate medial to lateral MI regions. Within hours of a peripheral nerve transection in adult rats, movements represented in neighboring MI areas are evoked from the cortical territory of the affected body part. One potential mechanism for reorganization is that adjacent cortical regions expand when preexisting lateral excitatory connections are unmasked by decreased intracortical inhibition. During pharmacological blockade of cortical inhibition in one part of the MI representation, movements of neighboring representations were evoked by stimulation in adjacent MI areas. These results suggest that intracortical connections form a substrate for reorganization of cortical maps and that inhibitory circuits are critically placed to maintain or readjust the form of cortical motor representations.

ALTHOUGH IT HAS BEEN ARGUED that the MI map is basically stable over time in adult animals (*1*), the possibility that MI continually reorganizes has been recognized since Sherrington's studies (*2*). The details of MI maps vary considerably in size and shape between animals, but the relative location of face, forelimb, and hindlimb areas is one consistent

Center for Neural Science, Box 1953, Brown University, Providence, RI 02912.